Journal of
Composites Science

MDPI

Article

Investigations on Structural and Optical Properties of Various Modifier Oxides (MO = ZnO, CdO, BaO, and PbO) Containing Bismuth Borate Lithium Glasses

J. Bhemarajam [1], P. Syam Prasad [2,*], M. Mohan Babu [2], Mutlu Özcan [3,*] and M. Prasad [1,*]

[1] Department of Physics, Osmania University, Hyderabad 500007, India; jadiphysics2012@gmail.com
[2] Department of Physics, National Institute of Technology Warangal, Warangal 506004, India; mmbabu771@gmail.com
[3] Center of Dental Medicine, Division of Dental Biomaterials, Clinic of Reconstructive Dentistry, University of Zurich, 8032 Zurich, Switzerland
* Correspondence: syam9405@gmail.com (P.S.P.); mutluozcan@hotmail.com (M.Ö.); prasad5336@yahoo.co.in (M.P.)

Abstract: Bismuth based quaternary glasses with compositions BiBLM: $50Bi_2O_3$–$20B_2O_3$–$15Li_2O$–15MO (where MO = ZnO, CdO, BaO, and PbO) were processed by conventional melt quenching. The effectiveness of various modifier oxides on the optical and structural properties of the developed glasses was studied systematically by XRD, DSC, FTIR, Raman, and optical absorption (OA) measurements. The synthesized glass specimens were characterized by XRD and the patterns demonstrated an amorphous nature. The physical characteristics such as molar mass, density, and OPD values were found to increase with an increase in the molar mass of the modifier oxides, while there was a decrement in oxygen molar volume, thus resulting in decrement of complete molar volume of the prepared glasses. From DSC analysis, incorrigible reduction and enhancement of T_g and thermal stability among various modifier oxides in the glass network was noticed. Optical absorption data for glass specimens have confirmed the decrease in both direct and indirect optical band gap values among various modifier oxides incorporation. These investigations support the obtained Urbach energy (UE) and metallization criteria of synthesized glasses. The ionic characteristic for the glass specimens were confirmed by the values of electronic polarizability and electronegativity. The Raman and FT-IR spectra of the glass specimens displayed the existence of BiO_3, BiO_6, ZnO_4, CdO_4, BaO_4, BO_3, PbO_4, and BO_4 structural units within the glass matrix. These structural results can support the applications of as-developed glasses in the area of photonics.

Keywords: bismuth glasses; modifier oxides; structural study; optical absorption; DSC; FTIR-Raman spectroscopy

check for updates

Citation: Bhemarajam, J.; Syam Prasad, P.; Mohan Babu, M.; Özcan, M.; Prasad, M. Investigations on Structural and Optical Properties of Various Modifier Oxides (MO = ZnO, CdO, BaO, and PbO) Containing Bismuth Borate Lithium Glasses. *J. Compos. Sci.* **2021**, *5*, 308. https://doi.org/10.3390/jcs5120308

Academic Editors: Francesco Tornabene and Thanasis Triantafillou

Received: 5 August 2021
Accepted: 4 November 2021
Published: 25 November 2021

Highlights

- Structural and Optical properties of the glasses were explored.
- The absence of crystallization peak in DSC clearly showed high thermal stability of glasses.
- The ionic nature of the glasses was identified from electronic polarizability and electronegativity.
- BiO_6, BiO_3, ZnO_4, CdO_4, BaO_4, PbO_4, BO_4, and BO_3 structural units were identified.

1. Introduction

Glasses, being amorphous in nature, exhibit optical isotropy. These transparent materials have received ample attention in the fields of science and technology [1]. For as far back as decade, many researchers have explored bismuth-contained glasses due to their remarkable advantages in the field of photonics and their application in optical isolators, infrared transmission components, optoelectronics, optical fiber amplifiers, laser

systems, ultrafast switches, and various photonic devices [2–5]. When borate is added to the bismuth glass network, it leads to larger optical basicity, a high refractive index, longer IR (infrared) cut-off, and second and third order non-linear optical susceptibility. These properties haveengrossed significant attention for their photonic and optoelectronic applications [6–8]. In addition, bismuth glasses containing alkali oxides (such as Li_2O, Na_2O etc.) possess high conductivity and act as ionic conductors compared to the other types of glasses [9]. Consequently, lithium bismuthate glasses are subject to a large edge-sharing BiO_n polyhedral. On the one hand, it is similar to a Bi_2O_4 crystal. On the other hand, BiO_6 polyhedra are found in the major construction units in these glasses. At the same time, the inclusion of small amountof Li_2O in bismuth glasses and lithium ions moves to structural interstates to replace the surplus of BiO_6 octahedral negative charge.

Borate, being the one of the strongest and main glass network formers among the other glass formers, has been paid great attention due to its exciting technological applications. In general, the B atoms coordinate with tri and tetra oxygen atoms in borate containing glasses, creating structural units of [BO_4] or [BO_3]. These structural units constitute (B–O–B) boran-oxygen-boran linkages that help to enhance the optical equities of the different glasses through prompting the bonds of M–O (metal-oxygen bonds) and NBOs (non-bridging oxygen atoms) [10,11]. Asmall field strength of about 0.53 of Bi^{3+} in B_2O_3 improves the optical and glass-forming ability. However, the addition of MO to the network system leads to a more compositional change, which results in increasing the refractive index of the NBOs [12–14]. Particularly, the addition of B_2O_3 can enhance the optical properties and glass-forming ability of bismuthate glass materials. Moreover, the refractive index of the bismuth-borate glasses is observed to be higher than quite a few other bismuth-based glasses. Hazra et al. investigated the structure of the Bi_2O_3 glass network (octahedral units of BiO_6 and pyramidal units of BiO_3) by IR and Raman techniques [15]. Fu and Yatsuda have studied the formation of glass and their optical followed by thermal properties of Bi_2O_3–MO and Bi_2O_3–Li_2O–MO glasses. Nitta et al. have reported the glass formation and thermal properties of Bi_2O_3–B_2O_3–Li_2O–MO glass systems. A bismuth-borate-based glass system was deliberated widely by many authors, who attempted to estimate their thermal, structural, and optical properties [16,17]. The incorporating of divalent ions such as Zn^{2+}, Cd^{2+}, Ba^{2+}, and Pb^{2+} to the high mole content of a bismuth oxide glass system played a significant role in improving its optical, structural, and physical properties [8–10,17]. Further, the addition of MO oxide to the Bi_2O_3–B_2O_3–Li_2O glass enhances the stability and polarizability of the ions in the network of glass. The analysis of the ternary glass system Bi_2O_3–B_2O_3–Li_2O–MO is of explicit interest due to the presence of more polarizability of bismuth and boron and, along with lithium and MO, could increase the nonlinear optical properties by increasing the refractive index of the glasses. It would also be significant to evaluate the structural deviation of the glass system due to the various modifier ions added to the bismuth glasses and to study the interaction behavior of the MO ions. MO contributes to the system of glasses through borate and bismuth, the initiation of oxygen three corners, and the lone electrons of borate (bismuth Bi^{3+} at the fourth corner restricts the third central way of the Bi atom). There might be a chance of borate ions within a B^{3+} state being devoted to a glass network starting with BO_4 accompanied with BiO_3 structural groups in glass systems. This could lead to the improvement of its the NLO (nonlinear optical) properties [12,15,18,19]. As of now, limited research is available regarding the optical and structural studies of different MO mixed bismuth borate lithium glasses. Moreover, the chosen host glass system contains more (50) % heavy metal oxide Bi_2O_3. When various MO (MO = ZnO, CdO, BaO, and PbO) are added to the HMO glass system, it can enhance the optical properties suitable for the development of photonic devices. The incorporation of HMO to the borate network along with the different modifier oxides are predicted to enhance and to reduce the multi phonon relaxation compared to other doped glass systems. Further, to the best of our knowledge, comprehensive and exhaustive studies on the structural and optical studies of HMO containing borate lithium glasses are marginally available in literature.

In the present work, we are dedicated in investigating the optical, thermal, and structural properties of the Bi_2O_3–B_2O_3–Li_2O–MO (MO = ZnO, CdO, BaO, and PbO) glass system with different modifier oxides by various characterization techniques to probe the suitability of these glasses as potential photonic materials.

2. Experimental Techniques

Glasses with a composition consisting of $50Bi_2O_3$–$20B_2O_3$–$15Li_2O$–15MO (MO = ZnO, CdO, BaO, and PbO) were synthesized by traditional melting and quenching techniques. High immaculateness of chemicals B_2O_3, Bi_2O_3, BaO, Li_2O, CdO, ZnO, and PbO, were procured from Sigma Aldrich to prepare the glasses. The requisite molecular % of the compounds have been taken and carefully grounded until the homogeneity is achieved. Then, the mixture is taken into a platinum crucible which is placed in muffle furnace to melt at 1000–1050 °C for one hour. The melt form of composition was then poured onto a pre-heated steel mold. The prepared glasses specimens were annealed at 300 °C about 3 h to relieve the internal stresses. These glasses are labelled as BiBLM glasses (BiBLM1(M1 = ZnO), BiBLM2 (M2 = CdO), BiBLM3 (M3 = BaO), and BiBLM4 (M4 = PbO)) and are visually transparent. The prepared BiBML glasses were initially characterized by XRD by Philips diffractometer (PANalytical X-pert-pro model, Malvern Panalytical, Malvern, UK) with radiation source Cu K_α (1.54 Å) and diffraction through an angle 2θ in the range 10° to 80° with a scan rate of 4°/min and step size of 0.02°. The DSC investigations were carried for all the specimens on DSC Q-20 instrument in the range of 100 °C to 700 °C temperatures at 10 °C/min rate.

The density of the BiBLM glasses were measured using Archimedes method, the captivation liquid as xylene (ρ = 0.86 g/cc). By using density values some physical parameters like molar volume (V_m) and V_m of oxygen followed by oxygen packing density (OPD) for the BiBLM glasses were evaluated. The optical absorption (OA) spectra of polished glasses specimens were noted within the wavelength range of 400–900 nm using a spectrometer (LABINDIA Instruments Pvt. Ltd., Mumbai, India) with 0.5 nm resolution. FTIR spectra of the glass samples were documented within the wavenumber range of 400–1600 cm^{-1} with 1 cm^{-1} resolution by Bruker ALPHA-II FTIR spectrometer (Bruker, Billerica, MA, USA) with the KBr pellet technique. Micro Raman Spectrometer (Renishaw Invia Reflex, Renishaw, Wotton-under-Edge, UK) measured Raman spectra for the BiBLM glass materials with 514.5 nm of Argon ion laser in the wavenumber between 100–1000 cm^{-1} under a backscattering arrangement.

3. Results and Discussion

3.1. Physical Parameters

Physical properties such as density (ρ), molar volume (V_m), and oxygen molar volume (V_o) followed by oxygen packing density (OPD) were evaluated for all glasses. The values are given in Table 1. The density of BiBLM glasses were evaluated from the Archimedes equation, and with an accuracy of 0.001 mg, using the formula below

$$\rho_g = \rho_{\text{xylene}} \times \frac{W_{\text{air}}}{W_{\text{air}} - W_{\text{xylene}}} \tag{1}$$

where W_{air} is the weight in an air medium, W_{xylene} is the weight of glass in a xylene medium, and ρ_{xylene} is the density of xylene.

The V_m, V_o and OPD values of BiBLMglasses were assessed from the density from the following equations,

$$V_m = \frac{\sum x_i M_i}{\rho_g} \tag{2}$$

$$V_o = \frac{V_m}{n_i x_i} \tag{3}$$

$$OPD = 1000 \times C \times \left(\frac{\rho}{M}\right) \quad (4)$$

where ρ is the glass density, (M_i or M) is molecular weight, x_i is molar fraction, n_i is oxygen atom number in each oxide constituent, and C is the oxygen atoms number per formula of the BiBLM glasses.

Table 1. Physical parameters of BiBLM glasses.

S.No	Parameter	BiBLM1	BiBLM2	BiBLM3	BiBLM4
1	Molar Mass, M (g/mol)	263.602	270.655	274.394	286.374
2	Density, ρ (g/cm^3) ±0.001	5.848	6.282	6.491	6.816
3	Molar volume, Vm(cm^3/mol) (±0.1)	45.076	43.084	42.272	42.015
4	Oxygen molar volume V_O (cm^3/mol)	18.782	17.951	17.613	17.506
5	Oxygen packing density (OPD) (g-atom/1)	53.243	55.705	56.775	57.122

The density values for BiBLM glasses increased within in the range 5.848 to 6.516 g cm^{-3} with various MO oxides in the network of glasses. The density of glasses specifies the compactness of the network of glasses. These values of density increasing due to increasing atomic radii and molecular weights of ingredient elements leads to a larger density of MO oxides in the BiBLM glasses [3,13,20]. The deliberate values of density of the glass specimens are reliable with analytical density values. On the other hand, there was inverse relation between values of molar volume and density of the glasses. The estimations of the V_o of the BiBLM glasses are originated to be decreasing due to the incorporation of different oxides in the present network, leading the highly packed local network to be loosened. This contrary behavior of OPD with oxygen molar volume is found as a result of the lower field intensity of different incorporation of MO oxides and is due ultimately to non-bridging oxygen atoms [13,20].

The organization between density and molar volume are displayed in Figure 1a. It is evident from the Figure 1a and Table 1, that density is increasing while molar volume is decreasing due to various modifier oxides in the composition of the present synthesized BiBLM glasses. At the same time from Figure 1b, the V_o and OPD follow the similar pattern i.e., BiBLM1 > BiBLM2 > BiBLM3 > BiBLM4. This may be due to the creation of non-bridging and bridging oxygen atoms which sit in the glass network.

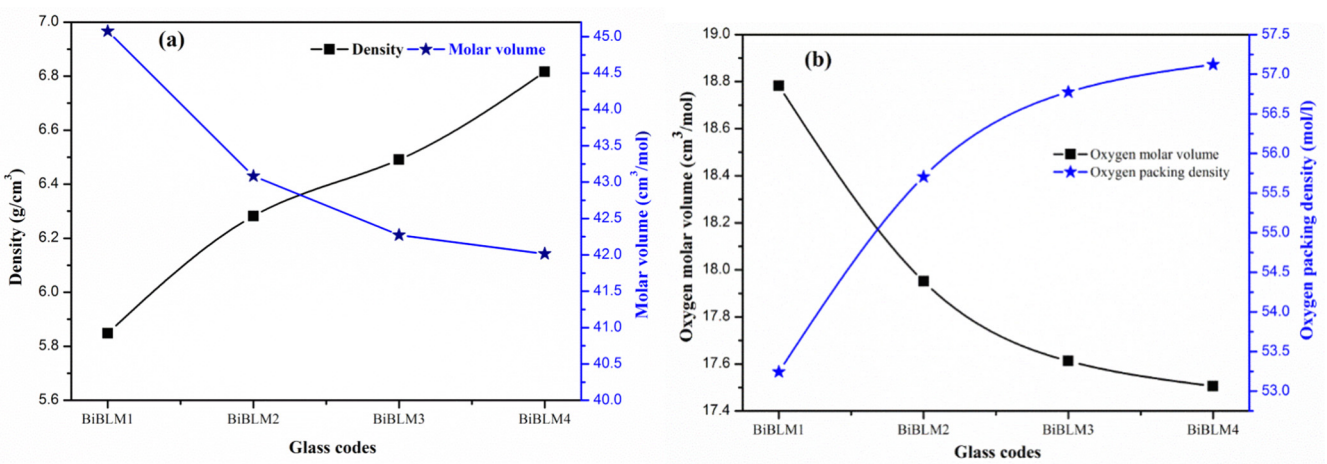

Figure 1. Association between (**a**) density (ρ) and molar volume (V_m), (**b**) oxygen molar volume (V_o) and oxygen packing density (OPD) with respect to the corresponding BiBLM glasses.

3.2. Thermal Analysis

The investigation of the thermal behavior of the glass accords significant evidence of structural features such as connectivity of local environment and steadiness of the glass.

The traces from the differential scanning calorimetry are used to evaluate the thermal properties of the as-prepared glasses.

The thermal behavior of BiBLM glasses is analyzed by DSC in the range of 100–700 °C and the results are presented in Figure 2a. The T_g (glass transition temperature), T_o (glass crystallization temperature), T_p (peak crystallization), and ΔT (thermal stability) values are noted in Table 2. It can be inferred from Table 2 that the glass transition temperature varies with the incorporation of different MO in BiBLM glasses. The T_g of glasses also depends on the density, as the density of the BiBLM glasses increases with the various modifier oxides by formation of Bi-O-MO linkages inside the glass matrix. It is noticed that the crystallization temperature of BiBLM3 glass system is nearly 420 °C and, except for the BiBLM3 glass, the DSC plots all other glasses (BiBLM1, BiBLM2 and BiBLM4) possess an exceptionally low tendency towards crystallization and trend more towards thermal stability [21]. From Table 2, it can be noticed that the value of T_g drops from 414 °C to 343 °C and then increases to 418 °C. This is mainly depending on the bond strengths between the atoms involved in the glass formation. The bond strength of B−O (498 kJ/mol) is hostile comparative to the bond strength of Bi−O bonds (102 kJ/mol). The bond strengths of Li–O (150 KJ/mol), Zn–O (151 kJ/mol), Ba–O (138 kJ/mol), Cd-O (84 kJ/mol) and Pb–O (101 kJ/mol) are responsible for decreasing in T_g values [22,23]. Further, the T_g of glasses also depends on the OPD of the glass system. With the addition of MO to the glass network, there is a change in OPD that leads to reduction in the glass transition temperature (T_g) [24,25]. In another way, the change occurred in T_g might be replacement of high strength of the metal-oxygen bond with low strength of metal-oxygen bond in the glass system. Furthermore, the increase in transition temperature T_g (418 °C) of BiBML4 is ascribed to the raise in density with MO constituent in the BiBML4 glass and also the bond energy of Ba–O (2.836 eV) is more than the Zn–O (2.714 eV). The strength of glass changes with the various MO in BiBML glasses is concluded and with the knowledge of Zn^{2+} (0.83 Å) which is lower cation radius is replaced with a higher cation radius of Cd^{2+} (1.03 Å), Pb^{2+} (1.35 Å) and Ba^{2+} (1.43 Å) [26]. The ΔT (T_0–T_g) is thermal stability, the ΔT value of BiBML1, BiBML2, BiBML3 and BiBML4 is found to be more than 100 °C, so the glasses formed are more rigid, highly cross-linked, and are very tightly packed in the network of the glasses. The increase in the thermal stability (as evidenced from OPD) of the BiBLM glasses is useful for the development of photonic devices like optical amplifiers, non-linear optical devices, etc. At the same time BiBLM4 glass has maximum T_g and thermal stability. So far, these are the best for analysis of luminance properties [27,28].

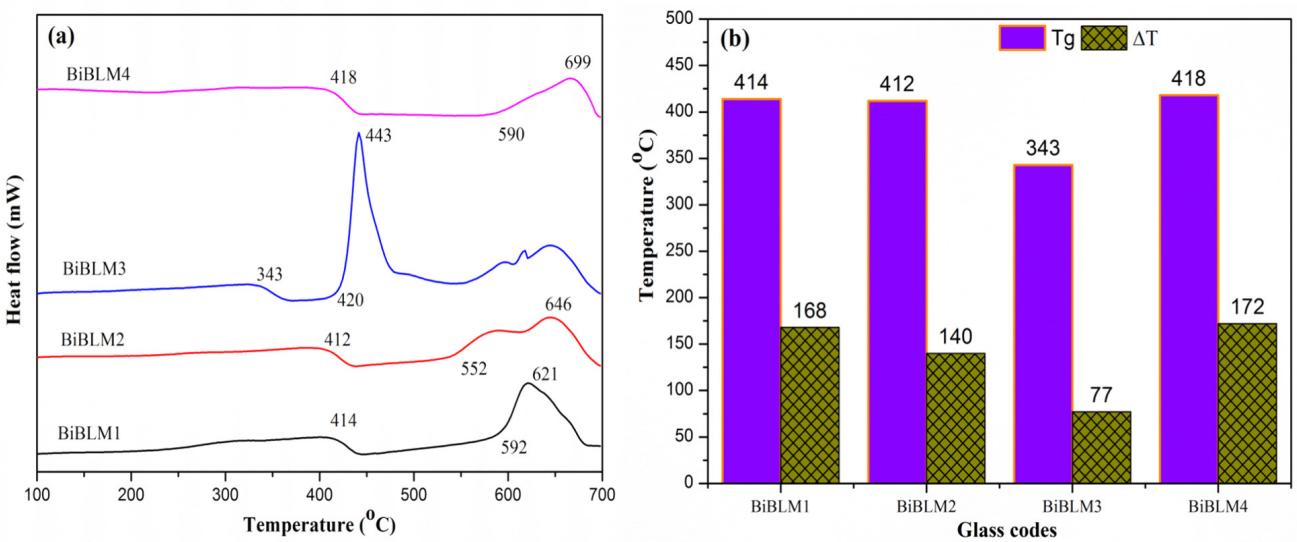

Figure 2. (**a**) DSC of BiBLM glass system; (**b**) compositional dependence of transition temperature (T_g) and thermal stability (ΔT) of BiBLM glass specimens.

Table 2. DSC parameters of BiBLM glasses.

Property	BiBLM1	BiBLM2	BiBLM3	BiBLM4
Glass transition temperature (T_g) (±1)	414	412	343	418
Glass Crystallization temperature (T_o) (±1)	592	552	420	590
Peak crystallization (T_p) (±1)	621	646	443	699
Thermal stability ΔT (T_o–T_g) (±1)	168	140	77	172

3.3. X-ray Diffraction

XRD studies as displayed in Figure 3, indicates the spectra of the amorphous nature of the synthesized BiBLM glass specimen. The traces of recorded XRD are contained a broad peak around 30° and missing of sharp peaks confirming the amorphous character of BiBLM1, BiBLM2, BiBLM3 and BiBLM4 glasses.

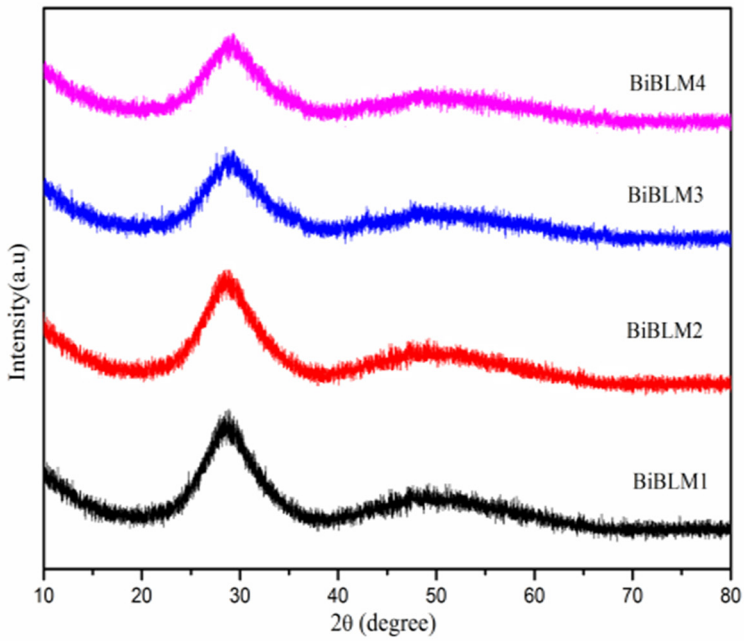

Figure 3. X-ray diffraction of BiBLM glass system.

3.4. FTIR Studies

FTIR analysis is apowerful technique forstudying the essential structural unit arrangement and functional groups presented in the materials. The spectra for the glass composition $50Bi_2O_3$–$20B_2O_3$–$15Li_2O$–15MO (MO= ZnO, CdO, BaO, and PbO) was displayed within the range of 400–1600 cm^{-1} at room temperature and are depicted in Figure 4. FTIR spectra disclosed the most significant structural studies of the glasses which tabulated in Table 3. Condrate et al., [29] described the structure of Bi_2O_3 based glasses as like that of crystalline α-Bi_2O_3. Although, the network of α-Bi_2O_3 is created by the continual linking of octahedral [BiO_6] and polyhedra [BiO_3] primary units by sharing corresponding vertices [23,30]. Consequently, the design of Bi_2O_3 primarily based glasses was developed by octahedral BiO_6 units related to collective corners. The Bi_2O_3 units were implicated that two oxygen along through a single pair of electrons. The equatorial position of Bi_2O_3 units in the bond length of the Bi–O bonds is slightly shorter than that of Bi–O axial bonds. The modes of vibrations borate are studied and categorized into three IR regions. The structure of borate glasses consists of di, tri, penta, pyro, metaborate, boroxol rings, and various modes of BO_3 and BO_4 groups. Generally, trigonal [BO_3] groups are ascribed to asymmetrical stretching vibrational modes of B–O bonds related to the first region at 1200–1600 cm^{-1}.

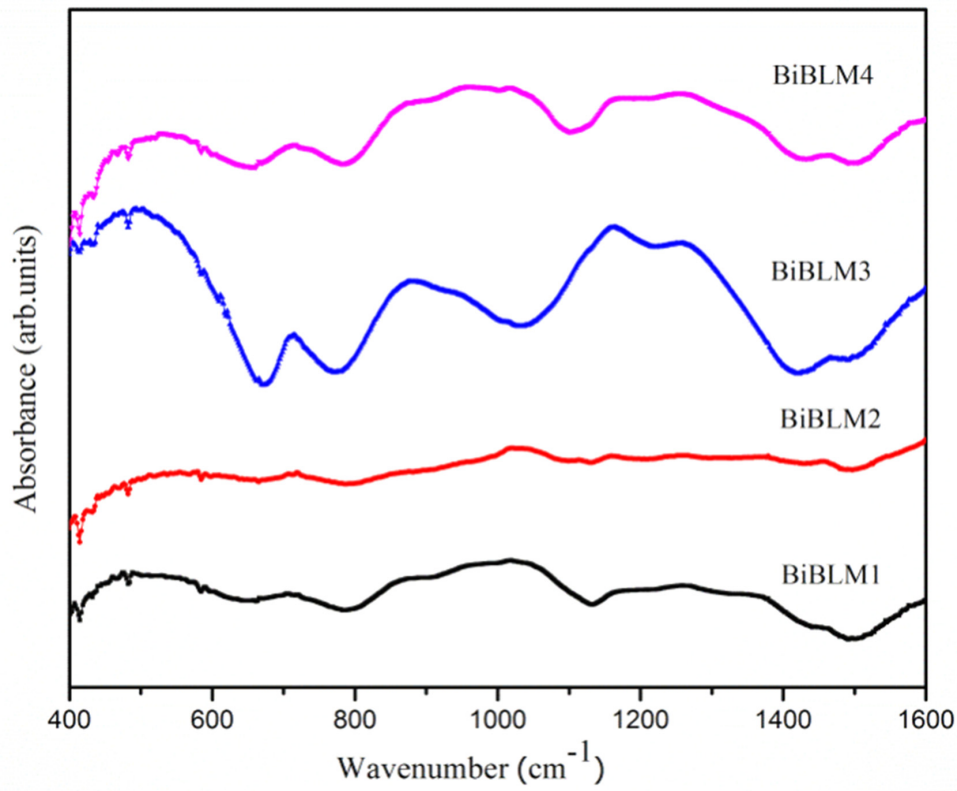

Figure 4. FTIR spectra of the BiBLM glasses.

Table 3. Assignment of FT-IR bands of BiBLM glasses.

Band Positions	Assignment
∼400–440	Bi−O bonds in distorted [BiO_6] octahedral units and a specific vibration of Li−O bonds.
∼440–460	Vibrations of Zn−O bonds from ZnO_4 tetrahedral, Vibrations of Cd-O bonds from CdO_4 tetrahedral vibration, Pb−O bonds from PbO_4 tetrahedral and bending vibrations of B−O−B linkages in BO_3 units.
∼560–592	Bi−O bending vibrations in the [BiO_6] octahedral units.
∼590–650	Stretching induced vibrations due to Bi−O^{-1} bonds which are mainly NBO's.
∼710–730	Chain-type metaborate, bending vibrations of B–O–B linkages in borate superposition of Bi−O bonds in the [BiO_3] pyramidal units to the B−O−B bending vibrations
∼750–770	Bending vibrations due to O_3B−O−BO_4 linkages.
∼850–870& ∼880–890	Characteristic vibrational bands of [BiO_3] polyhedral, symmetrical stretching induced vibrations in [BiO_3] units.
∼910	Stretching B−O vibrations in [BO_4] units from diborate groups
~1200–1270& ~1370, ~1380	Asymmetric stretching induced vibrations of B–O bond of trigonal [BO_3] units
∼1200–1300& ∼1500–1600	B−O stretching induced vibrations and overlapping of vibrations in [BO] units due to tri, tetra and penta borate groups and stretching induced vibrations in B−O bond in the [BO_3] units from boroxol rings.

Tetragonal [BO_4] groups are ascribed information of B–O band vibrations are stretching in the second region at 800–1200 cm^{-1} and other borate groups in B–O–B vibrations are bending in trigonal [BO_3] and tetrahedral [BO_4] group units in the third region at 400–800 cm^{-1} [2,21]. From the available literature, it is predicted that the vibrations induced bending in the range 400–600 cm^{-1} are octahedral [BiO_6] units due to Bi−O bands. Occasionally there occurs aconfusionon the inclusion of different MO and B_2O_3towards the Bismuth network, as these distinctive bands for bismuthate are essentially relative to B_2O_3. Appropriately, there might be few inclusions of the Bi−O groups with bending vibration of BO_3 units [9]. The prominent bands approximately at ∼406, ∼440, ∼445, ∼532, ∼541, and ∼597 cm^{-1} are credited to the broadening conveyed by vibrations induced bending of bands such as like Bi−O^{-1} and these are primarily presented as NBO (non-connecting

oxygen) atoms in polyhedral [BiO_6] units [31,32]. Also, a band at ∼440 cm^{-1} is ascribed to Bi−O bonds in octahedral units of bismuth [BiO_6], which are superposed by an IR bands because of specific vibrations of Li−O bonds [27,32]. The absorption bands at ∼620, ∼665, ∼710, ∼845, ∼867, and ∼878 cm^{-1} of the non-intricate data are often ascribed to assorted vibrations due to bending emerging in B−O−B bonds of the borate glass matrix [29] and Bi−O bonds in BiO_3 units [2,33]. There are various prominent peaks approximately at ∼705,∼710, and ∼725 cm^{-1}, and altogether the specimens that may be credited to the superstition of bands Bi−O and B in pyramidal [BiO_3] units of bending vibrations ($O_3B-O-BO_3$) [13,22]. The positioned peaks around ∼865 and ∼870 cm^{-1} are acknowledged as characteristic vibration bands due to Bi−O bonds in [BiO_3] polyhedral [22,34]. The peaks inferred in the range 860–1220 cm^{-1} are accredited to the induced stretching vibrations of B−O and extending of various arrangements in [BO_4] units due to the presence of various (tri, tetra, and penta) borate groups. A small deviation in wavenumber with chemical composition has been seen because of an increment in the [BO_4] units in the glass network [35,36]. The peak at 910 cm^{-1} is recognized as the fundamental peak promising due to induced stretching vibrations in B−O bonds of [BO_4] from diborate groups [4,30]. The peak prominent at around 1190 cm^{-1} can be intuited to asymmetric stretching induced vibrations due to B−O bonds of [BO_4] units from pyro and ortho borate groups [4]. The absorption peaks in the range of 1200–1600 cm^{-1} are ascribed to B−O the stretching induced vibrations which are developing in the [BO_3] units from the boroxol rings. The existence of boroxol rings have been accounted in borate containing binary, ternary, and quaternary glass networks. Moreover, these bands (B−O) are related to the vibrational modes inside the different borate rings and $B-O^{-1}$ bonds that are basically NBO atoms in nature. This may be attributed to enhance in the NBO atoms in borate rings [2].

3.5. Raman Spectra

Raman spectra of the BiBLM: $50Bi_2O_3$–$20B_2O_3$–$15Li_2O$–15MO (MO= ZnO, CdO, BaO and PbO) glasses were displayed in Figure 5 and the allotments of various bands are provided in Table 4. The vibrational Raman bands associated withthe various structural units for the present glass system are dominated by the heaviest cation bismuth (Bi^{3+}). Generally, the Raman bands due to Bi_2O_3 can be classified into four regions, i.e., low wave number Raman modes (<100 cm^{-1}), heavy metal ion vibrations (70–160 cm^{-1}), bridged anion modes in intermediate (300–600 cm^{-1}), and non-bridging anion modes at larger wave numbers [23,24]. The peaks within the range of 210 cm^{-1} to 240 cm^{-1} are endorsed to the vibrational modes of Bi−O in [BiO_3] as well as [BiO_6] units of glass network, andthe modes of Bi ions cause thesymmetry in stretching induced vibrations of Bi−O bonds [1,3,13,34]. The vibrational modes detected from 605 to 640 cm^{-1} are accredited to the $Bi-O^{-1}$ stretching induced vibrations in the units of [BiO_6] and also the vibration of meta-borate structural groups of ring nature structure. These vibrations also confirmed from the FTIR analysis that, as a shift of the bands from 400–600 cm^{-1}, which is due to the change of local symmetry in polyhedral [BiO_6]units as the MO into the system [1,13]. The presence of a Raman peak nearly about 260 cm^{-1} and FTIR bands in between 450 and 650 cm^{-1} are due to the presence of M−O tetrahedral bending vibrations in the BiBLM system [13,34,35]. Further, the peaks that are visible in the range between 940 cm^{-1} to 985 cm^{-1} may be licensed to the existence of modes of vibrations crediting to the B−O and B−O−B bonds present in the orthoborate and pyroborate group of [BO_3] triangular units [1,13,17,21,36–38]. In addition, the peaks ascribing to the band ranges from 1280 cm^{-1} to 1305 cm^{-1} are attributed to response of stretching induced vibrations of the $Bi-O^{-1}$ bonds, also at near 1320–1408 cm^{-1} shows the stretching vibrations of $Bi-O^{-1}$ bondsdue to the formation of NBOs, this is confirmed from the FTIR spectra which is ascribed by B−O−B [2,35,36]. Moreover, these bonds comprise of pyroborate groups and an ingredient of associated $Bi-O^{-1}$ groups. Also, many of the peaks were because of the vibrational bond modes taking in light of the vibrations in the B−O bonds in [BO_3] as well as [BO_4]

units [1,2,13,21,35,36]. The strong bands demonstrated near about 1280–1325 cm^{-1} are due to $Bi-O^{-1}$ stretching vibrations of $[BiO_3]$ units. The bands observed in FTIR spectra nearly at 850–890 cm^{-1} are due to symmetric stretching vibrations of $[BiO_3]$ and $[BiO_6]$ units and B−O−B bending vibrations of $[BO_3]$ units [2,13,35,36]. From this analysis, it has been concluded that on the incorporation of various modifiers in the glass network system causes the Raman shift of peaks from its present location, and the shifting may take place as an underlying variation to present glass system. The intensities of peaks are occurred due to the incorporating different oxides in the network. These are shown in Figure 5. A concise depiction of the assigning peaks of Raman is presented in Table 4.

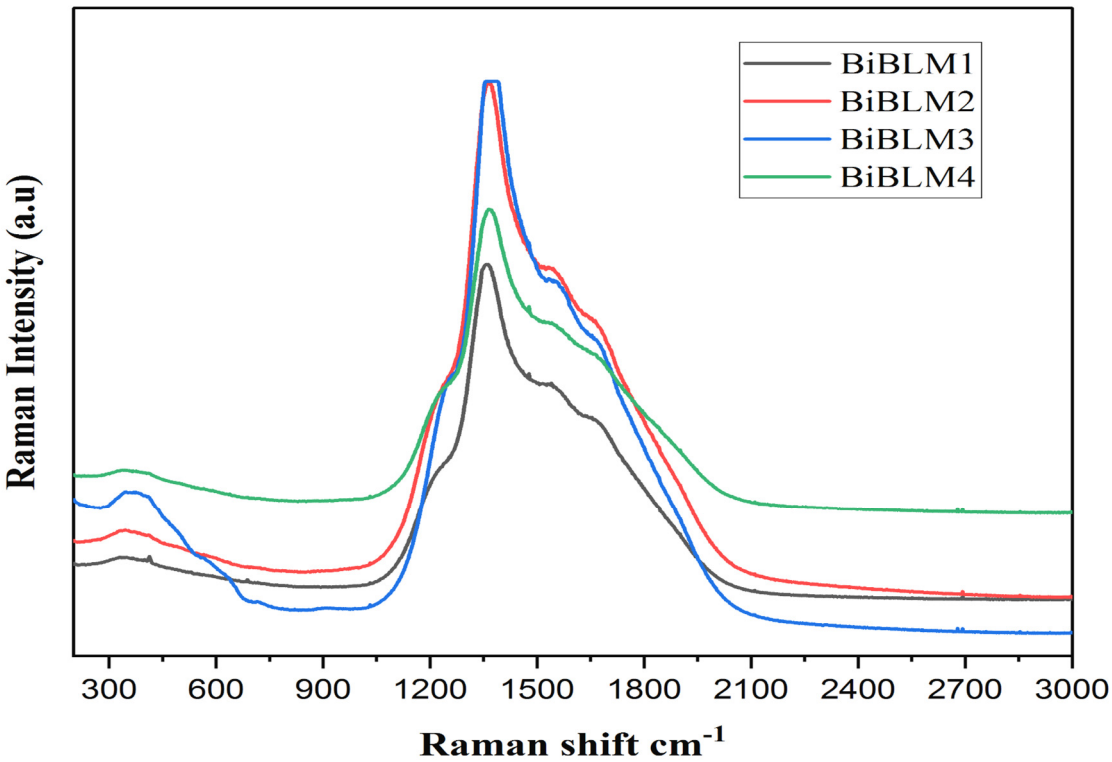

Figure 5. Raman spectra of the BiBLM glasses.

Table 4. Raman band assignment of BiBLM glasses.

Band Positions	Assignment
210–240	Vibrational modes of Bi−O in the $[BiO_3]$ and $[BiO_6]$ units
215–260	Modes of Bismuth ions due to symmetric stretching induced vibrations of Bi−O−Bi linkages in $[BiO_6]$ octahedral units
600–640	Bi−O−stretching induced vibrations in $[BiO_6]$ units and due to metaborate groups in ring structure and also due to B−O in $[BO_4]$ units or due to the linkages of M-O units
930–985	Vibrational modes occurring in the bonds like B−O and B−O−B in pyroborate groups of $[BO_3]$ units.
1280–1305	Stretching induced vibrations occurring in $Bi-O^{-1}$ bonds which are mainly considered as non bridging oxygen atoms.
1320–1408	Stretching induced vibrations occurring in $Bi-O^{-1}$ bonds which are mainly considered as non bridging oxygen atoms.

3.6. Optical Absorption (OA) Spectra

The estimation of OA recovers significant opto-structural studies of glasses. The OA spectra of BiBLM glasses are considered at room temperature and recorded the spectra within the range of 400–900 nm displayed in Figure 6. The chemical composition of the constituents in glass impacts the most part of the absorption edge and intensity. From Figure 6, the edges of the absorption for present glasses are absorbed in 417, 426, 435, and

449 nm for BiBLM1, BiBLM2, BiBLM3, and BiBLM4, respectively. The cut-off wavelengths (maximum intensity value in the absorption) of these glasses are estimated and given in Table 5. Cut-off wavelengths shifted towards higher wavelengths for the sample with different modifier oxides. It is also observed that the BiBLM1 glass has less cut-off wavelength value, whereas BiBLM4 has a high cut-off wavelength value compared to other glass specimens. The coefficient of absorption of prepared glasses is measured by using the equations mentioned in the reference [37].

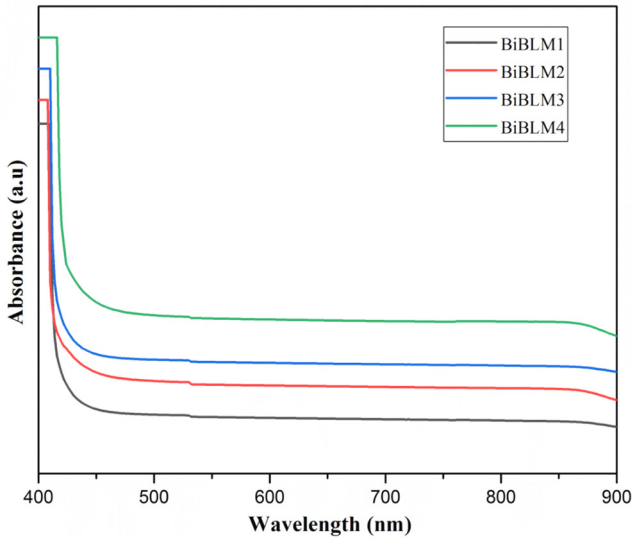

Figure 6. Optical absorption spectra of BiBLM glass system.

Table 5. Optical parameters of BiBLM glasses.

S.No	Parameter	BiBLM1	BiBLM2	BiBLM3	BiBLM4
1	Cut-off wavelength λ_c(nm) (±0.1)	417	426	435	449
2	Indirect band gap E_{ind}(eV) (±0.001)	1.931	1.7469	1.605	1.415
3	Direct band gap E_d(eV) (±0.001)	2.131	1.971	1.763	1.545
4	Urbach Energy ΔE(meV) (±0.001)	428	438	448	460
5	Molar refractivity Rm(cm^3)	23.951	22.946	22.630	22.581
6	Reflection losses R (%)	0.475	0.532	0.535	0.537
7	Metallization factor Mt	0.882	0.878	0.868	0.861
8	Refractive index n	2.098	2.102	2.111	2.118
9	Electronegativity (χ)	0.519	0.469	0.431	0.380
10	Electronic polarizability αe ($Å^3$)	3.033	3.078	3.112	3.158
11	Molar polarizability αm ($Å^3$)	9.504	9.105	8.980	8.961
12	Optical basicity (Λ)	1.441	1.465	1.484	1.509
13	Dielectric constant	4.402	4.412	4.456	4.486

3.6.1. Optical Band Gap and UrbachEnergy

The energy gap also referred to as bandgap energy (direct and indirect transition bandgaps) values of Bi_2O_3–B_2O_3–Li_2O–MO glasses can be calculated from the Mott and Davis relation [38] by using absorption coefficient α (v) and photon energy (hv).

$$\alpha(v) = B\left(\frac{hv - E_g}{hv}\right)^n \quad (5)$$

where hv indicates photon energy, E_g stands for optical energy gap, B is the band tailing parameter and 'n', the constant to evaluate the configuration of the optical transition. The values of 'n' equal to1/2 and 2 are direct and indirect allowed transitions, respectively. Tauc's calibrations [39] were sketched for $(\alpha hv)^{\frac{1}{n}}$ against energy of photon (hv)

by substituting the n values i.e., n = 1/2, 2 (direct and indirect allowed) electronic transition correspondingly. The respective plots are depicted in Figure 7a,b. The direct and indirect energy band gaps of BiBLM glasses were with $(\alpha hv)^2$ = 0 on X-axis for direct transition and $(\alpha hv)^{\frac{1}{2}} = 0$ for indirect transition correspondingly, and these are obtained from extrapolating the linear proportional part of the calibration. The values of indirect and direct optical band gaps of BiBLM glasses are displayed in Table 5. The obtained indirect and direct band gap values of BiBLM glasses are consistent with the other different bismuth borate glass [40]. From Figure 7a, the indirect band gap energy decreases from BiBLM1 to BiBLM4 (1.931 to 1.415 eV). Also absorbed from Figure 7b, direct energy band decreases from BiBLM1 to BiBLM4 (2.131 to 1.545 eV) due to different MO into the present glasses. This type of decrement in the values of energy band gaps suggests that rise in the number of NBO's in the present glasses with the addition of different modifier oxides [40]. From the FTIR analysis (in Section 3.4) it was confined that BiBLM glass comprises of the NBO's in the form of Bi–O, B–O, B–O–B, Bi–O–Bi, and B–O–B. As the inclusion of different MO (modifier oxides), the bridging oxygens are retrieved with NBOs because of higher basicity and polarizability of Bi_2O_3 [41]. Also, the values of bandgap energy of Bi-containing glasses (2.180–1.672 eV) are found to be smaller than different reported glasses i.e., Bi_2O_3–BaO–B_2O_3–Na_2O (4.41 to 4.68 eV) [42], alkali borate (3.11–3.21 eV) [43], and phospho-tellurite (3.232–3.343 eV) [44] glasses that suggested their impendency for the production of photonic devices.

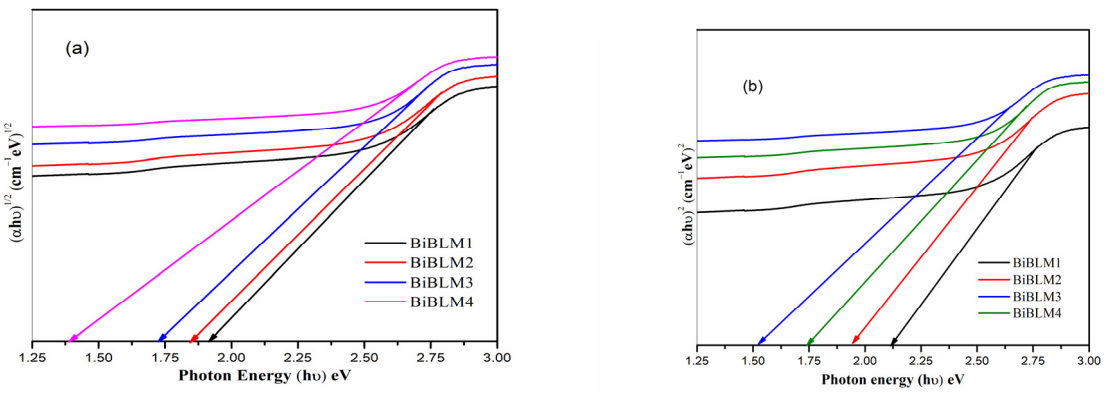

Figure 7. Tauc's plots (**a**) Indirect bandgap (**b**) direct bandgap of BiBML glasses.

Materials (amorphous), for instance, glasses incorporate a band stalking in the constrained energy band gap, these values implicate the minimal defects and disorderliness in the glasses, and these are evaluated using the Urbach rule [45,46].

$$\alpha\ (v) = \alpha_0 exp \frac{hv}{\Delta E} \tag{6}$$

where α_0 is a constant and ΔE represents the width of the band tails of an electron in different states in the forbidden band gap and these are known as the UE. The above Equation (6), also may be redrafted as

$$\ln \alpha(v) = \frac{hv}{\Delta E} + constant \tag{7}$$

The plots of $\ln \alpha$ are drawn across the hv (photon energy), these are known as Urbach plots. The UE values are accomplished by the reciprocal inverse of the slope of the linear curve of the plots as displayed in Figure 8, these values are given in Table 5. The UE of the BiBLM glasses is smaller than that of other Bismuthate containing glasses. UE of glasses increases from BiBLM1 to BiBLM4 (i.e., 428 to 460 meV), so that it suggests the presence of less disorderliness, minimum defects, and maybe in glasses system compositional changes take place in present glasses [47–50]. From Table 5 it is noticed that both indirect and direct

values follow the trend BiBLM1 > BiBLM2 > BiBLM3 > BiBLM4, also UE follows the reverse trend BiBLM4 > BiBLM3 > BiBLM2 > BiBLM1. This is due to band edge shifts towards the higher wavelength sides [47,50].

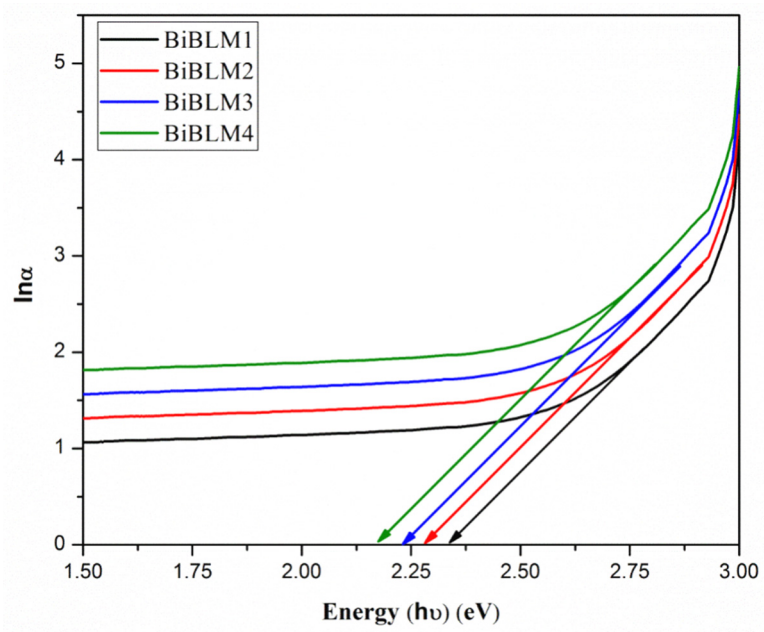

Figure 8. Urbach energy of BiBLM glasses.

3.6.2. Optical Properties

The molar refractivity (R_m) of the specimens was estimated with the help of the relation presented in Equation (8) [1,21,50].

$$R_m = V_m \left[1 - \sqrt{\frac{E_g}{20}} \right] \tag{8}$$

The molar refractivity (R_m) follows a linearly proportional relation with the molar polarizability (α_m) of the glass specimen material through the Lorentz-Lorentz equation as demonstrated in Equation (9) [21,51]. It signifies the number of electrons identified with an applied electrical field.

$$\alpha_m = \left(\frac{3}{4\pi N_A} \right) R_m \tag{9}$$

where N_A is Avogadro's number. In Table 5, it is observed that there is a decrease in the molar refractivity (R_m) and also a decrease in the molar polarizability (α_m) with various MO. It is also graphically illustrated in Figure 9a. In general, both (R_m) and (α_m) follow the same trend. For the present glasses, Rm decreases from BiBLM1 to BiBLM4 (23.951 to 22.581) and also α_m decreases from BiBLM1 to BiBLM4 (9.504 to 8.961) due to different MOs in the present glasses. This type of decrement in the values of Rm and α_m suggests that rise in the number of NBO's in the present glasses with the addition of different modifier oxides. Reflection loss (R_L) is derived from the ratio of molar volume and molar refractivity as displayed in Equation (10).

$$R_L = \frac{V_M}{R_M} \tag{10}$$

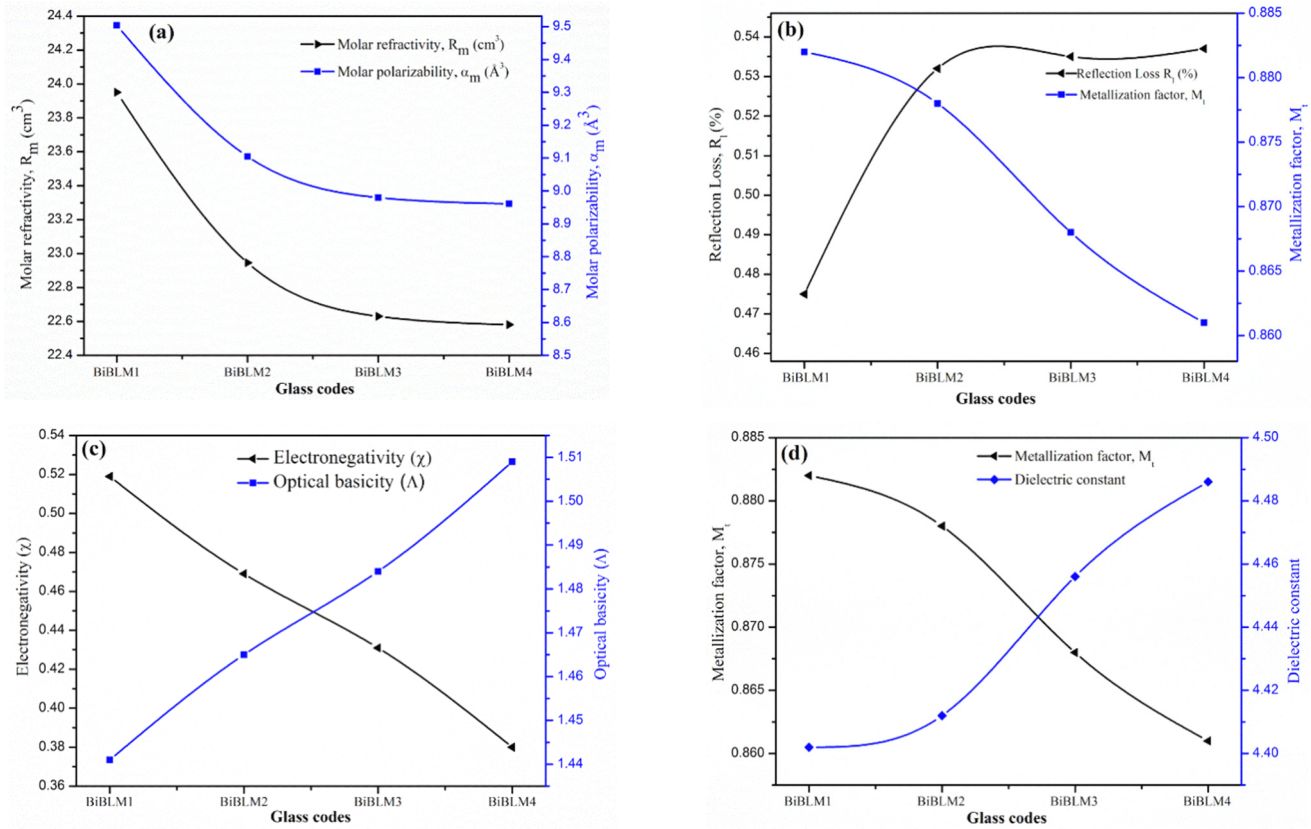

Figure 9. Dependence of (**a**) molar refractivity values (R_m) and electronic polarizability (α_e); (**b**) reflection loss R (%) and metallization factor (Mt), (**c**) electronegativity (χ) and optical basicity (Λ); (**d**) metallization factor (M_t) and dielectric constant corresponding to BiBLM glasses.

From the above formula, we have calculated the values of reflection loss and are increasing from 0.475 to 0.537 due to different MO incorporating in the glass system. The non-metallic nature of the materials can be characterized by metallization criteria [1,21]. These values depend onthe reflection loss values of the material. The metallization criterion can be calculated by following Equation (11),

$$\mathrm{M} = 1 - \frac{V_M}{R_M} \tag{11}$$

The Herzfeld theory explained about the metallization of condensed matter elucidates the fundamental state that non-metallic nature the materials possess (solid). For the Reflection loss (R_L) values approaching near to 1, then the material behaves has metal i.e., ($\frac{V_M}{R_M} > 1$), while the (R_L) values decrease and become smaller than 1 act as nonmetal i.e., ($\frac{V_M}{R_M} < 1$). In the current glass system, the values towards one (i.e., the reflection loss) has been found to linear with different MO in the network. The obtained values of metallization in the range of 0.882–0.861, so that these values are in harmony with optical non-linear performance and proposing the applications in various fields i.e., optical amplifiers and nonlinear devices [1,21]. From the table we noticed that values of R_L% increasing and M_t decreasing, which also displayed graphically in Figure 9b. From Figure 9b and Table 5, R_L follows BiBLM4 > BiBLM3 > BiBLM2 > BiBLM1 trend and M_t follows BiBLM1 > BiBLM2 > BiBLM3 > BiBLM4 trend due to creation of NBO atoms in the present network of the glass.

The refractive index (n) is evaluated with the help of reflection loss in Fresnel's formula using following Equation (12)

$$\frac{(n^2-1)}{(n^2+2)} = 1 - \sqrt{\frac{E_{opt}}{20}} \tag{12}$$

The refractive index is measured to examine the suitability of glass materials for the optical device. The refractive index of present synthesized glasses increases from BiBLM1 to BiBLM4 (i.e., 2.098 to 2.118) with different MO in the glasses. This also a result of the creation of new NBOs due to different polarizability of cations between M^{2+} (Zn^{2+} (0.28 Å^3), Cd^{2+} (1.05 Å^3), Ba^{2+} (1.59 Å^3) and Pb^{2+} (3.62 Å^3)) and Bi^{3+} (1.51 Å^3). The polarizability of the NBO atoms over the BO (bridging oxygen) atoms is useful for the more refractive index of the glasses. An ion's electronegativity is the intensity withwhich it absorbs electrons from the oxide ions bound to it. In this way, if the electronegativity of ion is bigger, it will incitethe fortified oxide ion so that it radiatesin close bonding between the network ions. By using the bandgap (E_g) values, the electronegative (χ) values of prepared glasses can be calculated. The following formula is used for the determination of optical electronegativity:

$$\chi = 0.2688E_g \tag{13}$$

The electronic polarizability (α_e) and optical basicity (Λ) are two significant factors, whichdepends on the electronegativity. These are estimated in accordance with the Dimitrov, Sakka, and Komatsu [32,33,52–56] stated correlations of electronegativity with the polarizability of cations and oxide optical basicity. The following two equations are useful for calculation of the electronic polarizability (α_e) and optical basicity (Λ) of the glasses.

$$\alpha_e = -0.9\chi + 3.5 \tag{14}$$

$$\Lambda = -0.5\,\chi + 1.7 \tag{15}$$

Both values of electronic polarizability (α_e) and optical basicity (Λ) are always greaterthan the opposite trend of electronegativity. The above-calculated values demonstratedthedecreasing of electronegativity due to different MO into glass network and at the same time increasing of the values of the electronic polarizability (α_e) and optical basicity (Λ). The calculated optical parameters are given in Table 5 and the related plots between electronegative(χ) and optical basicity (Λ) are illustrated in Figure 9c. From the Table 5 and Figure 9c, we perceived that (χ) follows the trend BiBLM1 > BiBLM2 > BiBLM3 > BiBLM4 and (Λ) shows the reverse trend (i.e., BiBLM4 > BiBLM3 > BiBLM2 > BiBLM1) due tothecreation of non-bridging oxygen sites. As suggested by Zhao et al. [53,56], Bi^{3+} cation possess very high polarizability, which is due to its large ionic radii and small cation unit field strength. Thus, the increasing the electron polarizability (α_0) and optical basicity (Λ) values of the present glasses on a molar basis can be attributed to the replacement of low polarizability of different MOs into the glass system. Hence, oxide ions are held tightly by Bi^{3+}. Consequently, a great overlapping arises among the O(2p) and Bi_2O_3 valence metal orbitals that aids theincrease of the covalent character very strongly between the Bi–O bond. In such instance of MO, the covering has occurred in the middle of O(2p) and valance metal orbits are smaller in composition to Bi_2O_3, this prompts less bond strength and impliesthat an ionic character can be exhibited among the chemical bonds. These outcomes are consistentwith the research findings of AXinyu Zhao, Dimitrov, Sakka, and P. Kaur [50,53,56–58]. Metal ions havemore humble electronegativity(χ) followed by bigger electron polarizability(α_e) with respect to bismuth ions, and thusthey can substitute B^{3+} ions with M^{2+} ions in present BiBLM glasses, which assists in expanding the ionic characteristic as a result of the more modest capability of M^{2+} ions, oxide ions clung to the tests. It is clear that for ionic chemical bond ages, at the expense of the covalent bonds, it is helpful to build the optical basicity for the current glasses with different MOs. Optical density is fundamentally the inclination of an oxide ion to add to the electron density of encompassing metal ions in the present

arranged glass system. It varies in an opposite way to deal with the metal-oxide bond strength. Likewise, upgrading the optical basicity among the aggregation of the MO in the glass is closely related to an evident lesser in the metal-oxide bond strength, and is therefore related to the decreased covalent nature and subordinate improved ionic nature. Its ionic nature proposes the formation of NBOs in the current glass matrix. This ionic nature and creation of NBOs in the glasses consistent with the reduction in the both direct and indirect band gaps investigation [27–29,57,58]. From the Table 5, also we noticed that M_t follows the BiBLM1 > BiBLM2 > BiBLM3 > BiBLM4 trend, at the same time reverse trend of dielectric constant of present glasses (i.e., BiBLM4 > BiBLM3 > BiBLM2 > BiBLM1 trend). It follow these trends due to the creation of the non-bridging oxygen atoms in the present synthesized glass system and the association between metallization factor (M_t) and dielectric constant, which are graphically illustrated in Figure 9d.

4. Conclusions

Bismuth borolithium glasses containing different modifier oxides were prepared successfully by the conventional melt quenching technique and their various structural properties were assessed to know the influence of modifier oxides on the host glass structure. Different physical parameters such as molar mass, density, and OPD values increased while the molar volume and oxygen molar volume of glasses decreased with different modifiers inclusion. The absence of crystallization peaks in the DSC curves represented the exceptionally high thermal stability of BiBLM glasses against crystallization. Among all modifiers, PbO mixed glasses (BiBLM4) showed the higher T_g and thermal stability. The amorphous nature is confirmed by XRD. FTIR and Raman analysis results revealed the transformation of structural units from $BiO_3 \rightarrow BiO_6$ in the glass system with the addition of various MO (modifier oxides). This transformation confirms that the character of bismuth with modifier oxides revealed the effective structural modifier of the glass system and employs the octahedral sites of the glass network. The different optical parameters such as optical band gaps, Urbach energy, metallization criterion, refractive index, electronic polarizability etc., follows either BiBLM4 > BiBLM3 > BiBLM2 > BiBLM1 or the reverse trend due to the formation of NBOs with the inclusion of various modifier oxides. In terms of physical, structural, and optical properties, the creation of NBOs in the glass network with addition of modifier oxides suggested the reduction in structural stability of the developed glass systems. These features of the glasses can be suitable for the generation of various photonic devices such as optical amplifiers, visible, and infrared up-converters, non-linear optical materials etc., used in the field of science and engineering.

Author Contributions: Data curation, J.B.; Formal analysis, M.M.B. and M.P.; Funding acquisition, M.Ö.; Investigation, J.B.; Methodology, J.B. and M.M.B.; Project administration, P.S.P., M.Ö. and M.P.; Resources, M.Ö.; Software, M.M.B.; Supervision, P.S.P. and M.P.; Validation, P.S.P.; Writing—original draft, J.B. All authors have read and agreed to the published version of the manuscript.

Funding: Article processing costs are funded by University of Zurich.

Acknowledgments: We are appreciative to OU-DST-PURSE-II Program (2017–2021) for monetary help to complete this research work. Authors additionally thank to Physics department, National Institute of Technology, Warangal for FT-IR spectroscopic analysis.

Conflicts of Interest: The authors declare no conflict of interest.

References

1. Alajerami, Y.S.M.; Hashim, S.; Hassan, W.M.S.W.; Ramli, A.T. The effect of titanium oxide on the optical properties of lithium potassium borate glass. *J. Mol. Struct.* **2012**, *1026*, 159–167. [CrossRef]
2. Singh, L.; Thakur, V.; Punia, R.; Kundu, R.S.; Singh, A. Structural and optical properties of barium titanate modified bismuth borate glasses. *Solid State Sci.* **2014**, *37*, 64–71. [CrossRef]
3. Farouk, M.; Samir, A.; Metawe, F.; Elokr, M. Optical absorption and structural studies of bismuth borate glasses containing Er^{3+} ions. *J. Non-Cryst. Solids* **2013**, *371–372*, 14–21. [CrossRef]

4. Park, J.; Kim, H.J.; Kim, S.; Cheon, J.; Kaewkhao, J. X-ray and proton Luminescences of bismuth-borate glasses. *J. Korean Phys. Soc.* **2011**, *59*, 657–660. [CrossRef]
5. Ardelean, I.; Cora, S.; Lucacel, R.C.; Hulpus, O. EPR and FT-IR spectroscopic studies of B_2O_3–Bi_2O_3–MnO glasses. *Solid State Sci.* **2005**, *7*, 1438–1442. [CrossRef]
6. Tagami, K.; Uchida, S. Transfer of REEs from nutrient solution to radish through fine roots and their distribution in the plant. *J. Alloy. Compd.* **2006**, *675*, 408–412. [CrossRef]
7. Kassab, L.R.P.; Junior, N.D.R.; Oliveira, S.L. Laser spectroscopy of Nd^{3+} doped PbO–Bi_2O_3–Ga_2O_3–BaO glasses. *J. Non-Cryst. Solids.* **2006**, *352*, 3224–3229. [CrossRef]
8. Boscaa, M.; Pop, L.; Borodi, G.; Pascuta, P. XRD and FTIR structural investigations of erbium-doped bismuth–lead–silver glasses and glass ceramics. *J. Alloy. Compd.* **2009**, *479*, 579–582. [CrossRef]
9. Murugan, G.; Varma, K. Characterization of lithium borate-bismuth tungstate glasses and glass-ceramics by impedance spectroscopy. *Solid State Ionics.* **2001**, *139*, 105–112. [CrossRef]
10. Prakash, D.; Seth, V.P.; Chned, I. Prem Chand, EPR study of vanadyl ion in CoO–PbO–B_2O_3 glasses. *J. Non-Cryst. Solids* **1996**, *204*, 46–52. [CrossRef]
11. Soliman, A.A.; Sakr, E.M.; Kashif, I. The investigation of the influence of lead oxide on the formation and on the structure of lithium diborate glasses. *Mater. Sci. Eng. B* **2009**, *158*, 30–34. [CrossRef]
12. Lee, S.; Hwang, S.; Cha, M.; Shin, H.; Kim, H. Role of Copper Ion in Preventing Silver Nanoparticles Forming in Bi_2O_3–B_2O_3–ZnO Glass. *J. Phys. Chem. Solids* **2008**, *69*, 1498–1500. [CrossRef]
13. Saritha, D.; Markandeya, Y.; Salagram, M.; Vithal, M.; Singh, A.K.; Bhikshamaiah, G. Effect of Bi_2O_3 on physical, optical and structural studies of ZnO–Bi_2O_3–B_2O_3 glasses. *J. Non-Cryst. Solids* **2008**, *354*, 5573–5579. [CrossRef]
14. Qiu, H.H.; Ito, T.; Sakata, H. DC Conductivity of Fe_2O_3–Bi_2O_3–B_2O_3 Glasses. *Mater. Chem. Phys.* **1999**, *58*, 243–248. [CrossRef]
15. Hazra, S.; Mandal, S.; Ghosh, A. Properties of unconventional lithium bismuthate glasses. *Phys. Rev. B* **1997**, *56*, 8021. [CrossRef]
16. Nitta, A.; Koide, M.; Matusita, K. Glass formation and thermal properties of Bi_2O_3–ZnO–B_2O_3–R_2O quaternary systems. *Phys. Chem. Glasses* **2001**, *42*, 275–278.
17. Griscom, D.L. Electron spin resonance in glasses. *J. Non Cryst. Solids* **1980**, *40*, 211–272. [CrossRef]
18. Friebele, E.J.; Uhlmann, D.R.; Kreidl, N.J. *Optical Properties of Glass*; American Ceramic Society: Westerville, OH, USA, 1991; pp. 205–262.
19. Sadeek, Y.B.; Shaaban, E.R.; Moustafa, E.S.; Moustafa, H.M. Spectroscopic properties, electronic polarizability, and optical basicity of Bi_2O_3–Li_2O–B_2O_3 glasses. *Phys. B* **2008**, *403*, 2399–2409. [CrossRef]
20. Moustafa, F.A.; Abdel-Baki, M.; Fayad, A.M.; El-diasty, F. Role of mixed valence effect and orbital hybridization on molar volume of heavy metal glass for ionic conduction pathways augmentation. *Am. J. Mater. Sci.* **2014**, *4*, 119–126.
21. Thakur, P.V.; Singh, A.; Punia, R.; Kaur, M.; Singh, L. Effect of $BaTiO_3$ on the structural and optical properties of lithium borate glasses. *Ceram. Int.* **2015**, *41*, 10957–10965. [CrossRef]
22. Shaaban, E.R.; Shapaan, M.; Saddeek, Y.B. Structural and thermal stability criteria of Bi_2O_3–B_2O_3 glasses. *J. Phys. Condens. Matter* **2008**, *20*, 155108. [CrossRef]
23. David, R.L. *CRC Handbook of Chemistry and Physics*; CRC: Boca Raton, FL, USA, 2004.
24. Journal, E.; Science, G.; Part, T. Synthesis, thermal and spectroscopic characterization of lithium bismuth borate glasses containing mixed transition metal ions. *Phys. Chem. Glasses Eur. J. Glass Sci. Technol. B* **2016**, *57*, 146–152.
25. Dimitrov, V.; Komatsu, T. An interpretation of optical properties of oxides and oxide glasses in terms of the electronic ion polarizability and average single bond strength. *J. Univ. Chem. Tech. Metall.* **2010**, *45*, 219–250.
26. Bhatia, B.; Meena, S.L.; Parihar, V.; Poonia, M. Optical basicity and polarizability of Nd^{3+}-doped bismuth borate glasses. *New J. Glass Ceram.* **2015**, *5*, 44–52. [CrossRef]
27. Laxmi Kanth, C.; Raghavaiah, B.V.; Appa Rao, B.; Veeraiah, N. Optical absorption, fluorescence and thermoluminescence properties of ZnF_2–MO–TeO_2 (MO = ZnO, CdO and PbO) glasses doped with Er^{3+} ions. *J. Lumin.* **2004**, *109*, 193–205. [CrossRef]
28. Yadav, A.; Dahiya, M.S.; Hooda, A.; Chand, P.; Khasa, S. Structural influence of mixed transition metal ions on lithium bismuth borate glasses. *Solid State Sci.* **2017**, *70*, 54–65. [CrossRef]
29. Robert, A.; Condrate, S. Vibrational spectra of structural units in glass. *J. Non-Cryst. Solids* **1986**, *84*, 26–33.
30. Laariedh, F.; Sayyed, M.I.; Kumar, A.; Tekin, H.O.; Kaur, R.; Badeche, T.-B. Studies on the structural, optical and radiation shielding properties of (50−x)PbO-10WO_3-10Na_2O-10MgO-(20+x)B_2O_3 glasses. *J. Non-Cryst. Solids* **2019**, *513*, 159–166. [CrossRef]
31. Bhemarajam, J.; Swapna; Babu, M.M.; Prasad, P.S.; Prasad, M. Spectroscopic studies on Er^{3+} ions incorporated bismuth borolead lithium glasses for solid state lasers and fiber amplifiers. *Opt. Mater* **2021**, *113*, 110818. [CrossRef]
32. Kaur, R.; Singh, S.; Pandey, O.P. Absorption spectroscopic studies on gamma irradiated bismuth borosilicate glasses. *J. Mol. Struct.* **2013**, *1049*, 386–391. [CrossRef]
33. Doweidar, H.; Saddeek, Y.B. FTIR and ultrasonic investigations on modified bismuth borate glasses. *J. Non-Cryst. Solids* **2009**, *355*, 348–354. [CrossRef]
34. Pascuta, P.; Borodi, G.; Culea, E. Structural investigation of bismuth borate glass ceramics containing gadolinium ions by X-ray diffraction and FTIR spectroscopy. *J. Mater. Sci. Mater. Electron.* **2009**, *20*, 360–365. [CrossRef]
35. Saddeek, Y.B.; Yahia, I.S.; Aly, K.A.; Dobrowolski, W. Spectroscopic, mechanical and magnetic characterization of some bismuth borate glasses containing gadolinium ions. *Solid State Sci.* **2010**, *12*, 1426–1434. [CrossRef]

36. Majhi, K.; Vaish, R.; Paramesh, G.; Varma, K.B.R. Electrical transport characteristics of ZnO–Bi_2O_3–B_2O_3 glasses. *Ionics* **2013**, *19*, 99–104. [CrossRef]
37. Mott, H.N.F.; Davis, E.A. *Electronic Processes in Non-Crystalline Materials*; Oxford University Press: Oxford, UK, 1974.
38. Davis, E.A.; Mott, N.F. Conduction in non-crystalline systems V. Conductivity, optical absorption and photoconductivity in amorphous semiconductors. *Philos. Mag.* **1970**, *22*, 903–922. [CrossRef]
39. Tauc, J.; Menth, A. States in the gap. *J. Non-Cryst. Solids* **1972**, *8–10*, 569–585. [CrossRef]
40. Duffy, J.A.; Ingram, M.D. Comments on the application of optical basicity to glass. *J. Non-Cryst. Solids* **1992**, *144*, 76–80. [CrossRef]
41. Abdel-Baki, M.; Fathy, A.; Abdel-Wahab; El-Diasty, F. One-photon band gap engineering of borate glass doped with ZnO for photonics applications. *J. Appl. Phys.* **2012**, *111*, 073506. [CrossRef]
42. Dogra, M.; Singh, K.J.; Kaur, K.; Anand, V.; Kaur, P.; Singh, P.; Bajwa, B.S. Investigation of gamma ray shielding, structural and dissolution rate properties of Bi_2O_3–BaO–B_2O_3–Na_2O glass system. *Radiat. Phys. Chem.* **2018**, *144*, 171–179. [CrossRef]
43. Mahesh, M.; Hivrekar; Sable, D.B.; Solunke, M.B.; Jadhav, K.M. Different property studies with network improvement of CdO doped alkali borate glass. *J. Non-Cryst. Solids* **2018**, *491*, 14–23.
44. Kaur, P.; Singha, K.J.; Thakur, S.; Singh, P.; Bajwa, B.S. Investigation of bismuth borate glass system modified with barium for structural and gamma-ray shielding properties. *Spectrochim. Acta Part A Mol. Biomol. Spectrosc.* **2019**, *206*, 367–377. [CrossRef] [PubMed]
45. Elbashir, B.O.; Sayyed, M.I.; Dong, M.G.; Elmahroug, Y.; Lakshminarayana, G.; Kityk, I.V. Characterization of Bi_2O_3–ZnO–B_2O_3 and TeO_2–ZnO–CdO–Li_2O–V_2O_5 glass systems for shielding gamma radiation using MCNP5 and Geant4 codes. *J. Phys. Chem. Solids* **2019**, *126*, 112–123. [CrossRef]
46. Urbach, L.F. The Long-Wavelength Edge of Photographic Sensitivity of the electronic Absorption of Solids. *Phy. Rev.* **1953**, *92*, 1324. [CrossRef]
47. Annapoorani, K.; Basavapoornima, C.; Murthy, N.S.; Marimuthu, K. Investigations on structural and luminescence behavior of Er^{3+} doped Lithium Zinc borate glasses for lasers and optical amplifier applications. *J. Non-Cryst. Solids* **2016**, *447*, 273–282. [CrossRef]
48. Mariyappan, M.; Arunkumar, S.; Marimuthu, K. Effect of Bi_2O_3 on the structural and spectroscopic properties of Sm^{3+} ions doped sodiumfluoroborate glasses. *J. Mol. Struct.* **2016**, *1105*, 214–224. [CrossRef]
49. Ayuni, D.J.N.; Halimah, M.K.; Talib, Z.; Sidek, H.A.A.; Daud, W.M.; Zaidan, W. Optical Properties of Ternary TeO_2–B_2O_3–ZnO Glass System. *IOP Conf. Ser. Mater. Sci. Eng.* **2011**, *17*, 012027. [CrossRef]
50. Chen, K.Y.; Nie, Q.; Xu, T.; Dai, S.; Wang, X.; Shen, X. A study of nonlinear optical properties in Bi_2O_3–WO_3–TeO_2 glasses. *J. Non. Cryst. Solids* **2008**, *354*, 3468–3472. [CrossRef]
51. Hathot, S.F. Study of some physical and optical properties of Bi_2O_3–TeO_2–V_2O_5 glasses. *Auatrallian J. Basic Appl. Sci.* **2017**, *11*, 171–178.
52. Dimitrov, S.V.; Komatsu, T. Correlation among electronegativity, cation polarizability, optical basicity and single bond strength of simple oxides. *J. Solid State Chem.* **2012**, *196*, 574–578. [CrossRef]
53. Zhao, A.; Wang, X.; Lin, H.; Wang, Z. Correlation among electronic polarizability, optical basicity and interaction parameter of Bi_2O_3–B_2O_3 glasses. *Phys. B* **2007**, *390*, 293–300. [CrossRef]
54. Shashidhar, B.; Srinivasa Rao, N.; Rahman, S. Spectroscopic studies of Bi_2O_3–Li_2O–ZnO–B_2O_3 glasses. *Solid State Sci.* **2008**, *10*, 326–331.
55. Dimitrov, V.; SakK, S. Electronic oxide polarizability and optical basicity of simple oxides. *J. Appl. Phys.* **1996**, *79*, 1736–1740. [CrossRef]
56. Zhao, F.X.; Wang, X.; Lin, H.; Wang, Z. A new approach to estimate refractive index, electronic polarizability, and optical basicity of binary oxide glasses. *Phys. B* **2008**, *403*, 2450–2460. [CrossRef]
57. Duffy, J.A. Ultraviolet transparency of glass: A chemical approach in terms of band theory, polarisability and electronegativity. *Phys. Chem. Glasses* **2001**, *42*, 151–157.
58. Thakur, S.; Thakur, V.; Kaur, A.; Singh, L. Structural, optical and thermal properties of nickel doped bismuth borate glasses. *J. Non-Cryst. Solids* **2019**, *512*, 60–71. [CrossRef]